PS/LPI Note 85-32
07. 11. 1985

OPTICS OF THE 4 MEV LIL-W SPECTROMETER

K. HÜBNER

1. INTRODUCTION

In order to measure the energy and the energy spread at the exit of buncher W, D. Warner proposed to install a temporary spectrometer. This note describes the spectrometer layout, the optics and the obtainable resolution.

2. LAYOUT AND COMPONENTS

Figure 1 shows the layout of the spectrometer being a temporary set-up downstream of converter target W and taking the place of the first accelerating section of LIL-W (AC 25) which is not yet installed.

The beam leaves the buncher W with about 4 MeV kinetic energy. It enters the solenoid SNT25 focusing the beam in both planes with a minimum focal length of 0.41 m. Simultaneously, the planes of oscillation are rotated by 57°. It is the only vertically focusing element downstream of the buncher. Appendix I gives more details about it.

After having passed the position and intensity monitor UMA 25)[1]) (sensitivity to beam position and intensity to be determined after cabling), the beam crosses the plane of the wire beam scanner WBS 25[2]) and is collimated by either one of the two holes in the copper block holding the converter target (CEP 25). The hole radius can be chosen to be either 2.5 mm or 1.0 mm[3]). The pulsed solenoid SNP 25 is not used for these measurements.

The longitudinal charge distribution in the 10 to 25 ns long beam pulse after the aperture limit is measured by the wall current monitor WCM.25.S (Type W, sensitivity about 4 V/A; 0.22 - 1300 MHz)[4].

The pure sector magnet BHZ 25.S deviates the beam by 45° and, therefore, introduces an energy dispersion. It focuses horizontally (f = 1.13 m) and slightly defocuses (f = 40 m) in the vertical plane due to the fringe field extending over about 0.1 m.

Figure 1 gives the magnetic length of the magnet not the mechanical length! The magnetic field had been measured at LAL[5] where the magnet was used in the test station of the front-end V[6].

After having passed a pumping manifold the beam traverses the SEM grid MSH 25.S before hitting a dump. The grid consists of 20 vertical foils with a horizontal pitch of 2 mm and about 0.1 mm distance between the foils. The length of a strip foil is 84mm[7]. The frame holding the strips is mounted such that the strip plane is 15 mm downwards of the SEM flange axis. The foils stay in the beam; no movement of the frame required. The box can also house slits preceding the SEM grid but we shall not mount them; at least not at the beginning.

The vacuum chambers have the standard 40 mm diameter except in the bending magnet where the old, large chamber is used.

The dump is built up from lead-blocks; one might add some Al to reduce backscatter.

3. OPTICS

3.1 Choice of layout

We had two choices:

i) put the SEM grid at the image*) of the hole (classical spectrometer solution);

ii) put the SEM grid at the image of the buncher output.

---

*) Image is defined as the place where a beam ellipse upright at the object become again upright.

Figure 2 shows the locus of the images in real space. The locus of the buncher exit image is drawn for maximum and for vanishing solenoid strength. The distance between the longitudinal centre of the target hole, identical to the target arm axis, and the magnet front face is the parameter L_6.

It can be seen that the SEM grid could not be placed at the hole image. Hence, it was placed at an image of the buncher exit where the transverse beam ellipse must be upright. Scrutinizing the resolution versus solenoid strength and versus L_6, and maximizing the working space around the SEM grid, it was decided to put the SEM grid at the image of buncher exit for L_6 = 1.75 m and for a solenoid field B_S which is 3/4 of the maximum. The beam ellipse at the exit of the buncher (end face last cell) was assumed to have an aspect ratio:

$$x_{max}/x'_{max} = \beta_i = 0.25 \text{ m},$$

as the most recent PARMELA calculations indicate[8)].

Table 1, 2 give the geometry in terms of a MAD output. The first part (Table 1) goes from the cathode of gun W to the intersection of the gun axis with the linac axis in the α-magnet; the second part (Table 2) starts from this intersection and ends at the plane of MSH.25.S. The length of the gun is equal to the distance from the cathode to the anode exit. The solenoid lengths are optical lengths (cf. Appendix 1) except for SNW23 where the mechanical length is given. For SNG221 and SNG222, the optical length refers to 60 keV kinetic energy, for SNT25, to 4 MeV kinetic energy. All solenoids are split to give the position of the centre for the survey. Table 3 gives the input to MAD which may be useful because it contains comments. Question marks in the comments indicate that the position of the element was measured on the drawings.

Although the longitudinal position of these elements is not critical, we would like to define it precisely. Otherwise our calculations can never model the reality. Since no better information is available, it is proposed that the positions so deduced become the nominal positions.

Elements occurring only once per section have on the drawings a two-digit number. Since MAD does not permit blanks in the element names, we add a 0. The LIL-W indicator WL. becomes W for lack of space and without loss of information. For example, the axis of the coupler at WL.PBW.22 becomes WPBW220C, the C indicating that this element designates a position and not a length. The steering coils DHZ are not given because they coincide with the steering coils DVT.

Some elements have numbers referring to a wrong section (WDVT221, WPBW220) but since they appear in this way on all drawings and lists of LIL it is preferred to make no changes.

Tables 4 and 5 give the geometry in the survey reference frame. Fig. 8 shows the accelerator reference frames. Appendix II gives the transformation from the gun-W and from the LIL-W reference frame to the survey reference system. The transformation from the LIL-W system ($z = 0$ at intersection of axes) to the rather odd LAL reference frame ($z = 0$ at end of LIL and z running against the beam) is also shown. This transformation is useful for checking against LAL drawings.

3.2 Momentum resolution

If $\beta_i \neq 0.25$ m and $B_S \neq 3/4\ B_{Smax}$, the SEM grid is "out of focus" and the ellipse at the SEM is tilted. This does not necessarily imply that the other settings give a larger horizontal beam size. This is illustrated for a beam of given emittance but different initial β_i in Fig. 3a and 3b. Note, the SEM grid only measures the projection onto the x-axis.

Figure 4 gives the horizontal half-size Δx of the beam versus B_S with β_i as parameter. We use $\varepsilon = 4\ \pi$ mm.mrad[8]) in agreement with the specifications $\varepsilon \leqslant 9\ \pi$ mm.mrad[9]). The initial aspect ratio β_i is varied by a factor 4 in both directions in order to see its influence. Obviously, the initially widest beam ($\beta_i = 1$ m) is also wider at the image.

Up to this point we have dealt with a mono-energetic beam. Since the dispersion function at the SEM grid is

$$D_x = \frac{dx}{dp/p} = 1.28 \text{ m}$$

a beam with vanishing emittance but with a momentum spread covers the width

$$\Delta x_e = D_x\ \Delta p/p$$

indicated for $\Delta p/p = 10^{-3}$ in Fig. 4. We define the momentum resolution $(\Delta p/p)_r$ as the momentum difference two non-zero emittance, mono-energetic beams must have in order to form two separate distributions along the x-axis at the SEM grid plane as sketched in Fig. 3c. Hence

$$(\Delta p/p)_r = 2\ \Delta x/D_x$$

However, in our case, it is more likely that Δx is always smaller than the 2 mm foil width, which becomes the effective resolution limit

$$(\Delta p/p)_r = 1.6 \times 10^{-3}$$

Figure 4 gives the upper limits for Δx. In reality, the beam is smaller because it is cut down by the target hole. This is apparent from Fig. 5 where the beam radius at the target hole is given.

But even if we neglect this fact it is clear from Fig. 4 that the resolution is determined by the foil width up to $\varepsilon \approx 11\ \pi$ µrad.m as long as we work with $B_s = 0$, which provides the best resolution. Hence, we did not bother to compute the real beam width due to the collimation by the hole.

3.3 Vertical Beam Size

The vertical plane is different. The half-width of the beam without collimation by the hole would reach 40 mm downstream of the 45° magnet exceeding the available aperture in the 20 mm radius vacuum chambers. Thus, we need to know the effect of the collimation. Fig. 6a sketches the effect of the target hole in the SEM grid phase plane. Only the hatched part of the beam arrives at the SEM grid and the beam height is reduced to Δy_{eff}.

Fig. 7a, 7b gives the final result for the nominal emittance and for twice the nominal emittance. We have taken into account that in some cases the beam is small enough to pass the hole (Fig. 6b) and other possible cases (Fig. 6c).

Inspection of Fig. 7 shows that the beam will easily pass through the vacuum pipe especially if $r_h = 1$ mm and small B_s are used.

4. DISCUSSION

The momentum spread desired is < 1%[9]. The resolution we can very likely get is about 0.16%, which is adequate. The absolute momentum measurement will be of the order of a few percent. The error is likely due to our ignorance of the true bending angle (effect of stray fields). But this precision is sufficient.

However, there is one problem. If the momentum spread exceeds 3.1%, the beam starts to hit the upstream 40 mm diameter orifice of the SEM grid box or the vacuum chamber. Two solutions exist:

i) the SEM box can house movable slits in front of the grid. This would allow for scanning the momentum spectrum by changing the strength of the bending magnet. Since the slits (SLH) are not planned to be ready in November, we would have to find a temporary solution by putting two fixed plates or a plate with a narrow window either into the SEM box or into the 40 mm diameter vacuum chamber just upstream of the SEM.

ii) the SEM box is moved closer to the bending magnet by shortening the pipe between pumping manifold and SEM box. This reduces D_x because $D_x' = 0{,}707$. Since the energy spectrum is then > 3%, the concomitant loss in resolution when Δx (beam width due to emittance) starts to exceed 2 mm (foil width) will be tolerable.

Since the PARMELA runs[8,10] predict momentum spreads between 5 and 10%, it is not unlikely that we have these problems with the beam width. However, we preferred to make the layout for high resolution for a large emittance beam because this is more demanding in space.

Having seen that the solenoid SNT 25 does neither improve the resolution nor does it help with the vertical beam size, its usefulness might be questioned. Nevertheless we like to have it in order to force more beam through the hole; also it might help to get an idea on the emittance though we do not yet know how to disentangle β_i and ε. Although no study has been made, it is certain that we would have a better chance to learn something about the emittance if we had the pulsed solenoid SNP 25 in addition to SNT 25.

ACKNOWLEDGEMENTS

D.J. Warner and A. Riche have read the manuscript and have made useful suggestions. J.C. Godot has checked the MAD lists against the drawings.

REFERENCES

1) S. Battisti, PS/LPI Note 83-11

2) M. Van Rooij and C. Steinbach, CERN/PS 85-33 (1985)

3) R. Bertolotto, priv. communication

4) E. Marcarini, priv. communication

5) M. Renard, Manuscript attached to memo by G. Le Meur, Note SA No. 10/81, 12.10.1981

6) P. Brunet and R. Chaput, Proc. Lin. Acc. Conf., Seeheim (1984) 189

7) S. Battisti, PS/LPI Note 83-17 (1983)
M. Van Rooij, priv. communication

8) J. Le Duff, Letter to K. Hübner (20.3.1984)
This calculation was done with a more realistic field than the first calculation[10]).

9) D. Warner, Note PS/LPI 82-10

10) Le Meur, Note LAL/PI 83-08/T (1983)

11) C. Fert and P. Durandeau in "Focusing of charged particles", Ed. A. Septier, Chapter 2.3 (1967)

12) K. Hübner, Note (31.5.1985)

REFERENCES

1) S. Battisti, PS/LPI Note 83-11

2) M. Van Rooij and C. Steinbach, CERN/PS 85-33 (1985)

3) R. Bertolotto, priv. communication

4) E. Marcarini, priv. communication

5) M. Renard, Manuscript attached to memo by G. Le Meur, Note SA No. 10/81, 12.10.1981

6) P. Brunet and R. Chaput, Proc. Lin. Acc. Conf., Seeheim (1984) 189

7) S. Battisti, PS/LPI Note 83-17 (1983)
M. Van Rooij, priv. communication

8) J. Le Duff, Letter to K. Hübner (20.3.1984)
This calculation was done with a more realistic field than the first calculation[10]).

9) D. Warner, Note PS/LPI 82-10

10) Le Meur, Note LAL/PI 83-08/T (1983)

11) C. Fert and P. Durandeau in "Focusing of charged particles", Ed. A. Septier, Chapter 2.3 (1967)

12) K. Hübner, Note (31.5.1985)

APPENDIX I

If object and image are far from the solenoid its focal length is given by[11])

$$f = \frac{4\ (B\rho)^2}{\int B_z^2\ dz} \qquad (1)$$

where Bρ - magnetic rigidity of the particle. The usual matrix formulation of the solenoid focusing used in our calculations implies

$$\frac{1}{f} = \frac{1}{L}\ \frac{\theta}{2}\ \sin\frac{\theta}{2} \qquad (2)$$

where the angle of rotation of the oscillation planes by the solenoid is

$$\theta = \frac{B_s\ L_s}{2\ (B\rho)} \qquad (3)$$

we further know

$$\theta = \frac{\int B_z\ dz}{(B\rho)} \qquad (4)$$

The integrals in (1) and (4) are either known from measurements or computations. Combining these equations gives

$$L_S = \frac{2\ (B\rho) \int B_z\ dz}{\int B_z^2\ dz}\ \sin\frac{\int Bz\ dz}{2\ (B\rho)} \qquad (5)$$

$$B_S = \frac{\int B_z^2\ dz}{2(B\rho)\ \sin\left[\int B_z dz/2\ (B\rho)\right]} \qquad (6)$$

For $\theta/2 \ll 1$

$$L_{S0} = (\int B_z\ dz)^2/\int B_z^2 dz \qquad (7)$$

$$B_{S0} = \int B_z^2\ dz/\int B_z dz \qquad (8)$$

POISSON computations[12]) yield for SNT25

$$\int B_Z = 1.49 \times 10^{-2}\ \mathrm{T.m}$$

$$\int B_Z^2 dz = 2.21 \times 10^{-3}\ \mathrm{T^2 \cdot m}$$

at maximum current. Hence from (5) and (6) at $(B\rho) = 1.495 \times 10^{-2}$ T•m corresponding to 4 MeV kinetic energy

$$L_S = 0.0962\ \mathrm{m}$$

$$B_S = 0.155\ \mathrm{T}$$

Note that B_S is not quite proportional to current and L_S weakly depends on the excitation current due to the sin in (5) and (6). Since the effect is small (4% at 1/4 of maximum current), we neglected it in the optics calculations. Saturation effects are negligible as $B < 0.3$ T in the iron.

For the geometry list (see Table 3) we use (7) to get a solenoid length independent of excitation

$$L_{S0} = 0.100\ \mathrm{m}.$$

The length of the solenoids SNG is determined in the same way.

B_{S0} and θ are proportional to current.

APPENDIX II

Fig. 8 gives a plan view of the acceelerator reference systems. The cathode is at $Z_g = 0$ and the intersection of the axes is at $Z = 0$. The LAL reference system is also indicated.

Any transformation into the survey system $\vec{x}_s$ can be decomposed into a rotation described by a matrix M and a translation vector $\vec{t}$ linking the two origins.

1. Gun-W system $\vec{x}_g$ to survey $\vec{x}_s$

$$\vec{x}_s = M\vec{x}_g + t \qquad \vec{x} = (x, y, z)$$

$$M = \begin{bmatrix} -0.99467641 & 0 & -0.10304817 \\ 0.10304817 & 0 & -0.99467641 \\ 0 & 1 & 0 \end{bmatrix} \quad t = \begin{bmatrix} 2207.95361 \\ 2067.26609 \\ 2433.5100 \end{bmatrix}$$

2. LIL-W system $\vec{x}$ to survey $\vec{x}_s$

$$M = \begin{bmatrix} 0.35697807 & 0 & -0.93411285 \\ 0.93411285 & 0 & 0.35697807 \\ 0 & 1 & 0 \end{bmatrix} \quad t = \begin{bmatrix} 2207.890748 \\ 2066.65934 \\ 2433.5100 \end{bmatrix}$$

3. LIL-W system $\vec{x}$ to LAL system $\vec{x}_L$

$$M = \begin{bmatrix} -1 & 0 & 0 \\ 0 & 1 & 0 \\ 0 & 0 & -1 \end{bmatrix} \qquad t = \begin{bmatrix} 0 \\ 0 \\ 64.8800 \end{bmatrix}$$

Distribution:

LAL:	LPI:	PS:	SPS:
P. Brunet	J.J. Aebi	B. Szeless	J.P. Quesnel
R. Chéhab	S. Battisti		
F. Dupont	A. Bellangero		
J. Le Duff	R. Bertolotto		
R. Belbéoch	D. Blechschmidt		
	J.P. Delahye		
	J.C. Godot		
	J.H.B. Madsen		
	B. Nicolai		
	A. Riche		
	D.J. Warner		

LIL W GEOMETRY OF OPTICAL ELEMENTS GUN W TO INTERSECTION WITH LIL "MAD" VERSION: 4.09 RUN: 04/11/85 18.12.07

SURVEY OF BEAM LINE "BLGWIL" PAGE 1

POS. NO.	ELEMENT NAME	OCC. NO.	SUM(L) [M]	ARC [M]	X [M]	Y [M]	Z [M]	THETA [RAD]	PHI [RAD]	PSI [RAD]
BEGIN	BLGWIL	1	0.0	0.0	0.0	0.0	0.0	0.0	0.0	0.0
BEGIN	BLL21	1	0.0	0.0	0.0	0.0	0.0	0.0	0.0	0.0
1	WGUN210	1	0.055000	0.055000	0.0	0.0	0.055000	0.0	0.0	0.0
2	WDRI211	1	0.096400	0.096400	0.0	0.0	0.096400	0.0	0.0	0.0
3	WDVT221U	1	0.116400	0.116400	0.0	0.0	0.116400	0.0	0.0	0.0
4	WDVT221D	1	0.136400	0.136400	0.0	0.0	0.136400	0.0	0.0	0.0
5	WDRI212	1	0.259000	0.259000	0.0	0.0	0.259000	0.0	0.0	0.0
END	BLL21	1	0.259000	0.259000	0.0	0.0	0.259000	0.0	0.0	0.0
BEGIN	BLL22U	1	0.259000	0.259000	0.0	0.0	0.259000	0.0	0.0	0.0
6	WDRI221	1	0.266500	0.266500	0.0	0.0	0.266500	0.0	0.0	0.0
7	WDIA220	1	0.266500	0.266500	0.0	0.0	0.266500	0.0	0.0	0.0
8	WDRI222	1	0.286600	0.286600	0.0	0.0	0.286600	0.0	0.0	0.0
9	WSNG221U	1	0.325000	0.325000	0.0	0.0	0.325000	0.0	0.0	0.0
10	WSNG221D	1	0.363400	0.363400	0.0	0.0	0.363400	0.0	0.0	0.0
11	WDRI223	1	0.365000	0.365000	0.0	0.0	0.365000	0.0	0.0	0.0
12	WWCM220U	1	0.417000	0.417000	0.0	0.0	0.417000	0.0	0.0	0.0
13	WWCM220D	1	0.469000	0.469000	0.0	0.0	0.469000	0.0	0.0	0.0
14	WDRI224	1	0.610000	0.610000	0.0	0.0	0.610000	0.0	0.0	0.0
15	WBHZ220C	1	0.610000	0.610000	0.0	0.0	0.610000	0.0	0.0	0.0
END	BLL22U	1	0.610000	0.610000	0.0	0.0	0.610000	0.0	0.0	0.0
END	BLGWIL	1	0.610000	0.610000	0.0	0.0	0.610000	0.0	0.0	0.0

TOTAL LENGTH = 0.610000 ARC LENGTH = 0.610000

ERROR(X) = 0.0 ERROR(Y) = 0.0 ERROR(Z) = 0.610000D+00

ERROR(THETA) = 0.0 ERROR(PHI) = 0.0 ERROR(PSI) = 0.0

Table 1

Gun W line

in Gun W reference frame

LIL W GEOMETRY OF OPTICAL ELEMENTS INTERSECTION AXES TO END SPECTR. "MAD" VERSION: 4.09 RUN: 04/11/85 18.12.07
SURVEY OF BEAM LINE "BLILS" PAGE 1

POS. NO.	ELEMENT NAME	OCC. NO.	SEQUENCE SUM(L) [M]	ARC [M]	POSITIONS X [M]	Y [M]	Z [M]	ANGLES THETA [RAD]	PHI [RAD]	PSI [RAD]
BEGIN	BLILS	1	0.0	0.0	0.0	0.0	0.0	0.0	0.0	0.0
BEGIN	BLILC	1	0.0	0.0	0.0	0.0	0.0	0.0	0.0	0.0
BEGIN	BLL22D	1	0.0	0.0	0.0	0.0	0.0	0.0	0.0	0.0
1	WBHZ220C	1	0.0	0.0	0.0	0.0	0.0	0.0	0.0	0.0
2	WDR1225	1	0.059500	0.059500	0.0	0.0	0.059500	0.0	0.0	0.0
3	WDVT222U	1	0.079500	0.079500	0.0	0.0	0.079500	0.0	0.0	0.0
4	WDVT222D	1	0.099500	0.099500	0.0	0.0	0.099500	0.0	0.0	0.0
5	WDR1226	1	0.153500	0.153500	0.0	0.0	0.153500	0.0	0.0	0.0
6	WSNG222U	1	0.191900	0.191900	0.0	0.0	0.191900	0.0	0.0	0.0
7	WSNG222D	1	0.230300	0.230300	0.0	0.0	0.230300	0.0	0.0	0.0
8	WDR1227	1	0.245000	0.245000	0.0	0.0	0.245000	0.0	0.0	0.0
9	WUMA220U	1	0.313000	0.313000	0.0	0.0	0.313000	0.0	0.0	0.0
10	WUMA220D	1	0.375000	0.375000	0.0	0.0	0.375000	0.0	0.0	0.0
11	WDR1228	1	0.404400	0.404400	0.0	0.0	0.404400	0.0	0.0	0.0
12	WDVT223U	1	0.424400	0.424400	0.0	0.0	0.424400	0.0	0.0	0.0
13	WDVT223D	1	0.444400	0.444400	0.0	0.0	0.444400	0.0	0.0	0.0
14	WDR1229	1	0.475000	0.475000	0.0	0.0	0.475000	0.0	0.0	0.0
END	BLL22D	1	0.475000	0.475000	0.0	0.0	0.475000	0.0	0.0	0.0
BEGIN	BLL23	1	0.475000	0.475000	0.0	0.0	0.475000	0.0	0.0	0.0
15	WDR1231	1	0.531000	0.531000	0.0	0.0	0.531000	0.0	0.0	0.0
16	WPBW220C	1	0.531000	0.531000	0.0	0.0	0.531000	0.0	0.0	0.0
17	WDR1232	1	0.585000	0.585000	0.0	0.0	0.585000	0.0	0.0	0.0
18	WSNG230U	1	0.623400	0.623400	0.0	0.0	0.623400	0.0	0.0	0.0
19	WSNG230D	1	0.661800	0.661800	0.0	0.0	0.661800	0.0	0.0	0.0
20	WDR1233	1	0.720800	0.720800	0.0	0.0	0.720800	0.0	0.0	0.0
21	WSNW230	1	1.014800	1.014800	0.0	0.0	1.014800	0.0	0.0	0.0
22	WDR1234	1	1.045000	1.045000	0.0	0.0	1.045000	0.0	0.0	0.0
23	WBNW230C	1	1.045000	1.045000	0.0	0.0	1.045000	0.0	0.0	0.0
24	WDR1235	1	1.258000	1.258000	0.0	0.0	1.258000	0.0	0.0	0.0
END	BLL23	1	1.258000	1.258000	0.0	0.0	1.258000	0.0	0.0	0.0
BEGIN	BLL25	1	1.258000	1.258000	0.0	0.0	1.258000	0.0	0.0	0.0
25	WDR1251	1	1.278300	1.278300	0.0	0.0	1.278300	0.0	0.0	0.0
26	WSNT250U	1	1.328500	1.328500	0.0	0.0	1.328500	0.0	0.0	0.0
27	WSNT250D	1	1.378700	1.378700	0.0	0.0	1.378700	0.0	0.0	0.0
28	WDR1252	1	1.408000	1.408000	0.0	0.0	1.408000	0.0	0.0	0.0
29	WUMA250U	1	1.476000	1.476000	0.0	0.0	1.476000	0.0	0.0	0.0
30	WUMA250D	1	1.538000	1.538000	0.0	0.0	1.538000	0.0	0.0	0.0
31	WDR1253	1	1.778500	1.778500	0.0	0.0	1.778500	0.0	0.0	0.0
32	WUPH250C	1	1.778500	1.778500	0.0	0.0	1.778500	0.0	0.0	0.0
33	WDR1254	1	1.941000	1.941000	0.0	0.0	1.941000	0.0	0.0	0.0
34	WWBS250C	1	1.941000	1.941000	0.0	0.0	1.941000	0.0	0.0	0.0
35	WDR1255	1	2.070000	2.070000	0.0	0.0	2.070000	0.0	0.0	0.0
36	WCEP250C	1	2.070000	2.070000	0.0	0.0	2.070000	0.0	0.0	0.0
37	WDR1256	1	2.071000	2.071000	0.0	0.0	2.071000	0.0	0.0	0.0
38	WCEP250	1	2.078000	2.078000	0.0	0.0	2.078000	0.0	0.0	0.0
END	BLL25	1	2.078000	2.078000	0.0	0.0	2.078000	0.0	0.0	0.0
END	BLILC	1	2.078000	2.078000	0.0	0.0	2.078000	0.0	0.0	0.0
BEGIN	BLLS	1	2.078000	2.078000	0.0	0.0	2.078000	0.0	0.0	0.0
39	WDR1257	1	3.490000	3.490000	0.0	0.0	3.490000	0.0	0.0	0.0
40	WWCM25SU	1	3.542000	3.542000	0.0	0.0	3.542000	0.0	0.0	0.0

Table 2 LIL-W injection line in LIL-W reference system

	ELEMENT	SEQUENCE			POSITIONS			ANGLES	
POS. NO.	ELEMENT NAME	OCC. NO.	SUM(L) [M]	ARC [M]	X [M]	Y [M]	Z [M]	THETA [RAD]	PHI [RAD]	PSI [RAD]
41	WWCM25SD	1	3.594000	3.594000	0.0	0.0	3.594000	0.0	0.0	0.0
42	WDRI258	1	3.820000	3.820000	0.0	0.0	3.820000	0.0	0.0	0.0
43	WBHZ25S	1	4.449600	4.449600	0.234792	0.0	4.386839	0.785398	0.0	0.0
44	WDRI259	1	5.929600	5.929600	1.281310	0.0	5.433357	0.785398	0.0	0.0
45	WMSH25SC	1	5.929600	5.929600	1.281310	0.0	5.433357	0.785398	0.0	0.0
END	BLLS	1	5.929600	5.929600	1.281310	0.0	5.433357	0.785398	0.0	0.0
END	BLILS	1	5.929600	5.929600	1.281310	0.0	5.433357	0.785398	0.0	0.0

TOTAL LENGTH = 5.929600 ARC LENGTH = 5.929600
ERROR(X) = 0.128131D+01 ERROR(Y) = 0.0 ERROR(Z) = 0.543336D+01
ERROR(THETA) = 0.785398D+00 ERROR(PHI) = 0.0 ERROR(PSI) = 0.0

Table 2 *continued*

```
TITLE
LIL - W    Geometry of optical elements    Gun W to spectrometer end     04.11.85
WGUN210    : DRIFT, L=0.0550                    ! CATHODE TO ANODE EXIT +- 1MM
WDRI211    : DRIFT, L=0.0414
WDVT221U   : HKICK, L=0.0200                    !?LENGTH OF YOKE
WDVT221D   : HKICK, L=0.0200                    !?LENGTH OF YOKE
WDRI212    : DRIFT, L=0.1226                    !-
WDRI221    : DRIFT, L=0.0075
WDIA220    : MARKER                             ! DIAPHRAGMA L=+- 1MM, R=12.5 MM
WDRI222    : DRIFT, L=0.0201
WSNG221U   : SOLENOID, L=0.0384, KS=2.731   ! OPTICAL LENGTH AT 60 KEV
WSNG221D   : SOLENOID, L=0.0384, KS=2.731   ! OPTICAL LENGTH AT 60 KEV
WDRI223    : DRIFT, L=0.0016
WWCM220U   : MONITOR,  L=0.0520                 ! MECH. LENGTH + 2MM FOR HALF-GASKET
WWCM220D   : MONITOR,  L=0.0520                 ! MECH. LENGTH + 2MM FOR HALF-GASKET
WDRI224    : DRIFT, L=0.1410
WBHZ220C   : MARKER                             !-INTERSECTION OF AXES  ANGLE=75.DEGR
WDRI225    : DRIFT, L=0.0595
WDVT222U   : HKICK, L=0.020                     !?LENGTH OF YOKE
WDVT222D   : HKICK, L=0.020                     !?LENGTH OF YOKE
WDRI226    : DRIFT, L=0.0540
WSNG222U   : SOLENOID, L=0.0384, KS=2.731   !?OPTICAL LENGTH
WSNG222D   : SOLENOID, L=0.0384, KS=2.731   !?OPTICAL LENGTH
WDRI227    : DRIFT, L=0.0147
WUMA220U   : MONITOR,  L=0.0680                 ! MECH. LENGTH + 2MM FOR HALF-GASKET
WUMA220D   : MONITOR,  L=0.0620                 ! MECH. LENGTH + 2MM FOR HALF-GASKET
WDRI228    : DRIFT, L=0.0294
WDVT223U   : HKICK, L=0.0200                    !?LENGTH OF YOKE
WDVT223D   : HKICK, L=0.0200                    !?LENGTH OF YOKE
WDRI229    : DRIFT, L=0.0306                    !
WDRI231    : DRIFT, L=0.0560
WPBW220C   : MARKER                             ! COUPLER AXIS PBW220
WDRI232    : DRIFT, L=0.0540
WSNG230U   : SOLENOID, L=0.0384, KS=2.731   !?OPTICAL LENGTH AT 60 KEV
WSNG230D   : SOLENOID, L=0.0384, KS=2.731   !?OPTICAL LENGTH AT 60 KEV
WDRI233    : DRIFT, L=0.0590
WSNW230    : DRIFT, L=0.2940                    ! LENGTH OF IRON YOKE
WDRI234    : DRIFT, L=0.0302
WBNW230C   : MARKER                             ! COUPLER AXIS BNW230
WDRI235    : DRIFT, L=0.2130                    !-
WDRI251    : DRIFT, L=0.0203
WSNT250D   : SOLENOID, L=0.0502, KS=1.      !?OPTICAL LENGTH AT 4 MEV
WSNT250U   : SOLENOID, L=0.0502, KS=1.      !?OPTICAL LENGTH AT 4 MEV
WDRI252    : DRIFT, L=0.0293
WUMA250U   : MONITOR,  L=0.0680                 ! MECH. LENGTH + 2MM FOR HALF-GASKET
WUMA250D   : MONITOR,  L=0.0620                 ! MECH. LENGTH + 2MM FOR HALF-GASKET
WDRI253    : DRIFT, L=0.2405
WUPH250C   : MARKER                             !?COUPLER AXIS OF UPH 25
WDRI 254   : DRIFT, L=0.1625
WWBS250C   : MONITOR                            ! CENTRE WIRE
WDRI255    : DRIFT, L=0.1290
WCEP250C   : MARKER                             ! CENTRE TARGET ARM
WDRI256    : DRIFT, L=0.0010
WCEP250    : DRIFT, L=0.0070                    !-CONVERTER TARGET
WDRI257    : DRIFT, L=1.4120
WWCM25SU   : MONITOR,  L=0.0520                 ! MECH. LENGTH + 2MM FOR HALF-GASKET
WWCM25SD   : MONITOR,  L=0.0520                 ! MECH. LENGTH + 2MM FOR HALF-GASKET
WDRI258    : DRIFT, L=0.2260

WBHZ25S    : SBEND, L=0.6296,ANGLE=-0.785398   ! OPTICAL LENGTH
WDRI259    : DRIFT, L=1.48
WMSH25SC   : MONITOR
```

Table 3

Sequence and lengths of elements (MAD input)

LIL W GEOMETRY OF OPTICAL ELEMENTS GUN W TO INTERSECTION WITH LIL "MAD" VERSION: 4.09 RUN: 04/11/85 18.12.07
SURVEY OF BEAM LINE "BLGWIL" PAGE 1

POS. NO.	ELEMENT NAME	OCC. NO.	SEQUENCE SUM(L) [M]	ARC [M]	POSITIONS X [M]	Y [M]	Z [M]	ANGLES THETA [RAD]	PHI [RAD]	PSI [RAD]
BEGIN	BLGWIL	1	0.0	0.0	2207.953607	2067.266091	2433.510000	[illegible]89	-1.467565	0.0
BEGIN	BLL21	1	0.0	0.0	2207.953607	2067.266091	2433.510000	4.712389	-1.467565	0.0
1	WGUN210	1	0.055000	0.055000	2207.947939	2067.211384	2433.510000	4.712389	-1.467565	0.0
2	WDRI211	1	0.096400	0.096400	2207.943673	2067.170204	2433.510000	4.712389	-1.467565	0.0
3	WDVT221U	1	0.116400	0.116400	2207.941612	2067.150311	2433.510000	4.712389	-1.467565	0.0
4	WDVT221D	1	0.136400	0.136400	2207.939551	2067.130417	2433.510000	4.712389	-1.467565	0.0
5	WDRI212	1	0.259000	0.259000	2207.926918	2067.008470	2433.510000	4.712389	-1.467565	0.0
END	BLL21	1	0.259000	0.259000	2207.926918	2067.008470	2433.510000	4.712389	-1.467565	0.0
BEGIN	BLL22U	1	0.259000	0.259000	2207.926918	2067.008470	2433.510000	4.712389	-1.467565	0.0
6	WDRI221	1	0.266500	0.266500	2207.926145	2067.001010	2433.510000	4.712389	-1.467565	0.0
7	WDIA220	1	0.266500	0.266500	2207.926145	2067.001010	2433.510000	4.712389	-1.467565	0.0
8	WDRI222	1	0.286600	0.286600	2207.924074	2066.981017	2433.510000	4.712389	-1.467565	0.0
9	WSNG221U	1	0.325000	0.325000	2207.920117	2066.942821	2433.510000	4.712389	-1.467565	0.0
10	WSNG221D	1	0.363400	0.363400	2207.916159	2066.904626	2433.510000	4.712389	-1.467565	0.0
11	WDRI223	1	0.365000	0.365000	2207.915995	2066.903034	2433.510000	4.712389	-1.467565	0.0
12	WWCM220U	1	0.417000	0.417000	2207.910636	2066.851311	2433.510000	4.712389	-1.467565	0.0
13	WWCM220D	1	0.469000	0.469000	2207.905278	2066.799588	2433.510000	4.712389	-1.467565	0.0
14	WDRI224	1	0.610000	0.610000	2207.890748	2066.659338	2433.510000	4.712389	-1.467565	0.0
15	WBHZ220C	1	0.610000	0.610000	2207.890748	2066.659338	2433.510000	4.712389	-1.467565	0.0
END	BLL22U	1	0.610000	0.610000	2207.890748	2066.659338	2433.510000	4.712389	-1.467565	0.0
END	BLGWIL	1	0.610000	0.610000	2207.890748	2066.659338	2433.510000	4.712389	-1.467565	0.0

TOTAL LENGTH =	0.610000	ARC LENGTH =	0.610000		
ERROR(X) =	-0.628591D-01	ERROR(Y) =	-0.606753D+00	ERROR(Z) =	-0.244995D-10
ERROR(THETA) =	0.137668D-13	ERROR(PHI) =	0.0	ERROR(PSI) =	0.0

Table 4

Gun W Line

in CERN survey reference frame

LIL W GEOMETRY OF OPTICAL ELEMENTS INTERSECTION AXES TO END SPECTR. "MAD" VERSION: 4.09 RUN: 04/11/85 18.12.07
SURVEY OF BEAM LINE "BLILS" PAGE 1

POS. NO.	ELEMENT NAME	OCC. NO.	SEQUENCE SUM(L) [M]	SEQUENCE ARC [M]	POSITIONS X [M]	POSITIONS Y [M]	POSITIONS Z [M]	ANGLES THETA [RAD]	ANGLES PHI [RAD]	ANGLES PSI [RAD]
BEGIN	BLILS	1	0.0	0.0	2207.890748	2066.659340	2433.510000	4.712389	0.365031	0.0
BEGIN	BLILC	1	0.0	0.0	2207.890748	2066.659340	2433.510000	4.712389	0.365031	0.0
BEGIN	BLL22D	1	0.0	0.0	2207.890748	2066.659340	2433.510000	4.712389	0.365031	0.0
1	WBHZ220C	1	0.0	0.0	2207.890748	2066.659340	2433.510000	4.712389	0.365031	0.0
2	WDRI225	1	0.059500	0.059500	2207.835168	2066.680580	2433.510000	4.712389	0.365031	0.0
3	WDVT222U	1	0.079500	0.079500	2207.816486	2066.687720	2433.510000	4.712389	0.365031	0.0
4	WDVT222D	1	0.099500	0.099500	2207.797804	2066.694859	2433.510000	4.712389	0.365031	0.0
5	WDRI226	1	0.153500	0.153500	2207.747362	2066.714136	2433.510000	4.712389	0.365031	0.0
6	WSNG222U	1	0.191900	0.191900	2207.711492	2066.727844	2433.510000	4.712389	0.365031	0.0
7	WSNG222D	1	0.230300	0.230300	2207.675622	2066.741552	2433.510000	4.712389	0.365031	0.0
8	WDRI227	1	0.245000	0.245000	2207.661890	2066.746800	2433.510000	4.712389	0.365031	0.0
9	WUMA220U	1	0.313000	0.313000	2207.598371	2066.771074	2433.510000	4.712389	0.365031	0.0
10	WUMA220D	1	0.375000	0.375000	2207.540456	2066.793207	2433.510000	4.712389	0.365031	0.0
11	WDRI228	1	0.404400	0.404400	2207.512993	2066.803702	2433.510000	4.712389	0.365031	0.0
12	WDVT223U	1	0.424400	0.424400	2207.494311	2066.810841	2433.510000	4.712389	0.365031	0.0
13	WDVT223D	1	0.444400	0.444400	2207.475628	2066.817981	2433.510000	4.712389	0.365031	0.0
14	WDRI229	1	0.475000	0.475000	2207.447044	2066.828905	2433.510000	4.712389	0.365031	0.0
END	BLL22D	1	0.475000	0.475000	2207.447044	2066.828905	2433.510000	4.712389	0.365031	0.0
BEGIN	BLL23	1	0.475000	0.475000	2207.447044	2066.828905	2433.510000	4.712389	0.365031	0.0
15	WDRI231	1	0.531000	0.531000	2207.394734	2066.848895	2433.510000	4.712389	0.365031	0.0
16	WPBW220C	1	0.531000	0.531000	2207.394734	2066.848895	2433.510000	4.712389	0.365031	0.0
17	WDRI232	1	0.585000	0.585000	2207.344292	2066.868172	2433.510000	4.712389	0.365031	0.0
18	WSNG230U	1	0.623400	0.623400	2207.308422	2066.881880	2433.510000	4.712389	0.365031	0.0
19	WSNG230D	1	0.661800	0.661800	2207.272552	2066.895588	2433.510000	4.712389	0.365031	0.0
20	WDRI233	1	0.720800	0.720800	2207.217440	2066.916650	2433.510000	4.712389	0.365031	0.0
21	WSNW230	1	1.014800	1.014800	2206.942810	2067.021601	2433.510000	4.712389	0.365031	0.0
22	WDRI234	1	1.045000	1.045000	2206.914600	2067.032382	2433.510000	4.712389	0.365031	0.0
23	WBNW230C	1	1.045000	1.045000	2206.914600	2067.032382	2433.510000	4.712389	0.365031	0.0
24	WDRI235	1	1.258000	1.258000	2206.715634	2067.108418	2433.510000	4.712389	0.365031	0.0
END	BLL23	1	1.258000	1.258000	2206.715634	2067.108418	2433.510000	4.712389	0.365031	0.0
BEGIN	BLL25	1	1.258000	1.258000	2206.715634	2067.108418	2433.510000	4.712389	0.365031	0.0
25	WDRI251	1	1.278300	1.278300	2206.696672	2067.115665	2433.510000	4.712389	0.365031	0.0
26	WSNT250U	1	1.328500	1.328500	2206.649779	2067.133585	2433.510000	4.712389	0.365031	0.0
27	WSNT250D	1	1.378700	1.378700	2206.602887	2067.151506	2433.510000	4.712389	0.365031	0.0
28	WDRI252	1	1.408000	1.408000	2206.575517	2067.161965	2433.510000	4.712389	0.365031	0.0
29	WUMA250U	1	1.476000	1.476000	2206.511998	2067.186240	2433.510000	4.712389	0.365031	0.0
30	WUMA250D	1	1.538000	1.538000	2206.454083	2067.208372	2433.510000	4.712389	0.365031	0.0
31	WDRI253	1	1.778500	1.778500	2206.229428	2067.294225	2433.510000	4.712389	0.365031	0.0
32	WUPH250C	1	1.778500	1.778500	2206.229428	2067.294225	2433.510000	4.712389	0.365031	0.0
33	WDRI254	1	1.941000	1.941000	2206.077635	2067.352234	2433.510000	4.712389	0.365031	0.0
34	WWBS250C	1	1.941000	1.941000	2206.077635	2067.352234	2433.510000	4.712389	0.365031	0.0
35	WDRI255	1	2.070000	2.070000	2205.957135	2067.398285	2433.510000	4.712389	0.365031	0.0
36	WCEP250C	1	2.070000	2.070000	2205.957135	2067.398285	2433.510000	4.712389	0.365031	0.0
37	WDRI256	1	2.071000	2.071000	2205.956200	2067.398642	2433.510000	4.712389	0.365031	0.0
38	WCEP250	1	2.078000	2.078000	2205.949662	2067.401140	2433.510000	4.712389	0.365031	0.0
END	BLL25	1	2.078000	2.078000	2205.949662	2067.401140	2433.510000	4.712389	0.365031	0.0
END	BLILC	1	2.078000	2.078000	2205.949662	2067.401140	2433.510000	4.712389	0.365031	0.0
BEGIN	BLLS	1	2.078000	2.078000	2205.949662	2067.401140	2433.510000	4.712389	0.365031	0.0
39	WDRI257	1	3.490000	3.490000	2204.630694	2067.905193	2433.510000	4.712389	0.365031	0.0
40	WWCM25SU	1	3.542000	3.542000	2204.582121	2067.923756	2433.510000	4.712389	0.365031	0.0

Table 5 LIL-W injection line
in CERN survey reference system

LIL W GEOMETRY OF OPTICAL ELEMENTS INTERSECTION AXES TO END SPECTR. "MAD" VERSION: 4.09 RUN: 04/11/85 18.12.07
SURVEY OF BEAM LINE "BLILS" PAGE 2

POS. NO.	ELEMENT NAME	OCC. NO.	SUM(L) [M]	ARC [M]	X [M]	Y [M]	Z [M]	THETA [RAD]	PHI [RAD]	PSI [RAD]
41	WWCM25SD	1	3.594000	3.594000	2204.533547	2067.942319	2433.510000	4.712389	0.365031	0.0
42	WDRI258	1	3.820000	3.820000	2204.322437	2068.022996	2433.510000	4.712389	0.365031	0.0
43	WBHZ25S	1	4.449600	4.449600	2203.792945	2068.225345	2433.744792	5.531840	0.255182	-0.263922
44	WDRI259	1	5.929600	5.929600	2202.815379	2068.598929	2434.791310	5.531840	0.255182	-0.263922
45	WMSH25SC	1	5.929600	5.929600	2202.815379	2068.598929	2434.791310	5.531840	0.255182	-0.263922
END	BLLS	1	5.929600	5.929600	2202.815379	2068.598929	2434.791310	5.531840	0.255182	-0.263922
END	BLILS	1	5.929600	5.929600	2202.815379	2068.598929	2434.791310	5.531840	0.255182	-0.263922

TOTAL LENGTH =	5.929600	ARC LENGTH =	5.929600		
ERROR(X) =	-0.507537D+01	ERROR(Y) =	0.193959D+01	ERROR(Z) =	0.128131D+01
ERROR(THETA) =	0.819451D+00	ERROR(PHI) =	-0.109849D+00	ERROR(PSI) =	-0.263922D+00

Table 5 continued

7

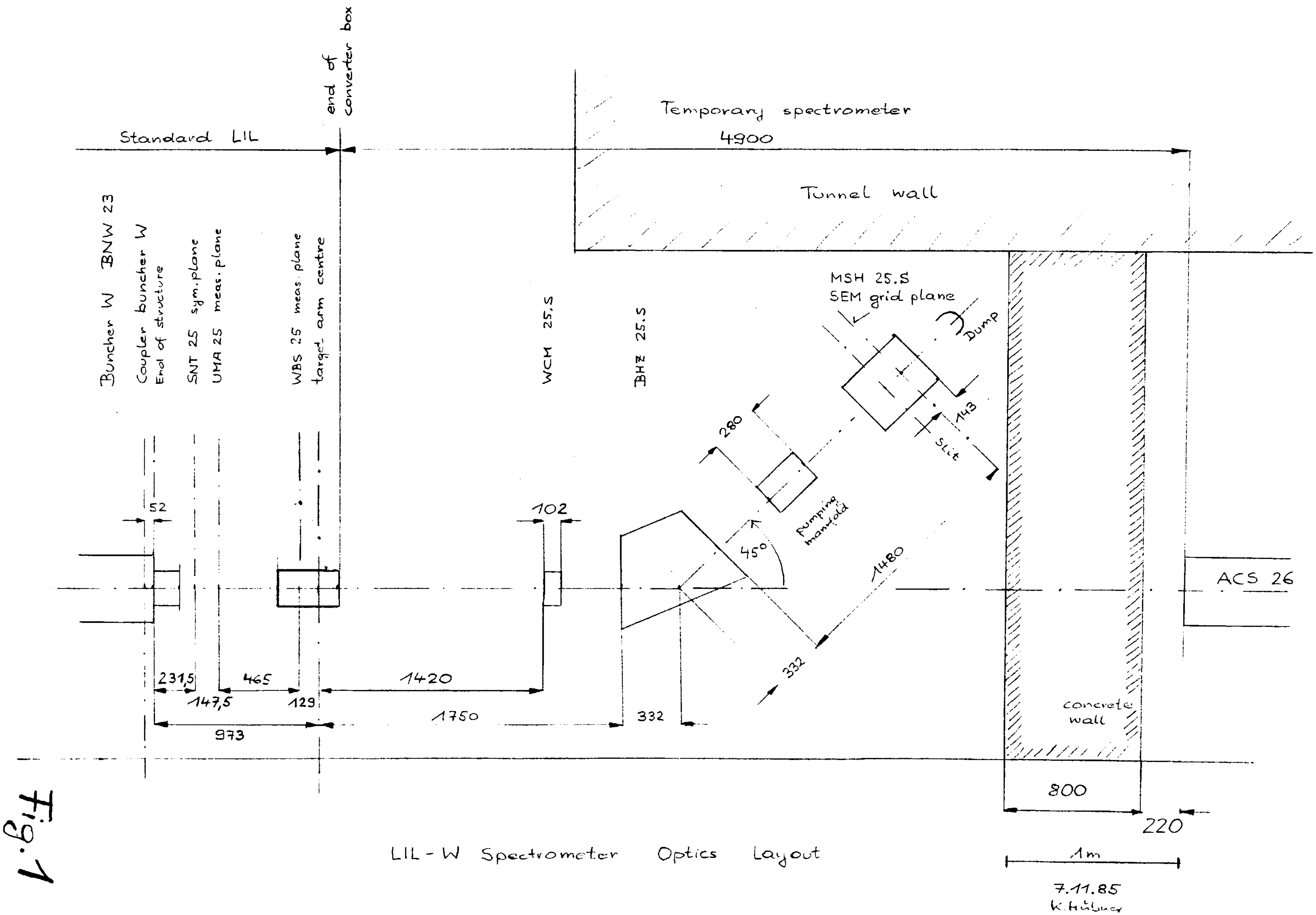
end of converter box
Standard LIL
Temporary spectrometer
4900
Tunnel wall
Buncher W BNW 23
Coupler buncher W
End of structure
SNT 25 sym.plane
UMA 25 meas.plane
WBS 25 meas.plane
target arm centre
WCM 25.S
BHZ 25.S
MSH 25.S
SEM grid plane
Dump
143
Slit
280
pumping manifold
45°
1480
332
52
102
ACS 26
231,5
465
1420
147,5
129
1750
332
973
concrete wall
800
220
LIL-W Spectrometer Optics Layout
1m
7.11.85
K. Hübner

Fig.1

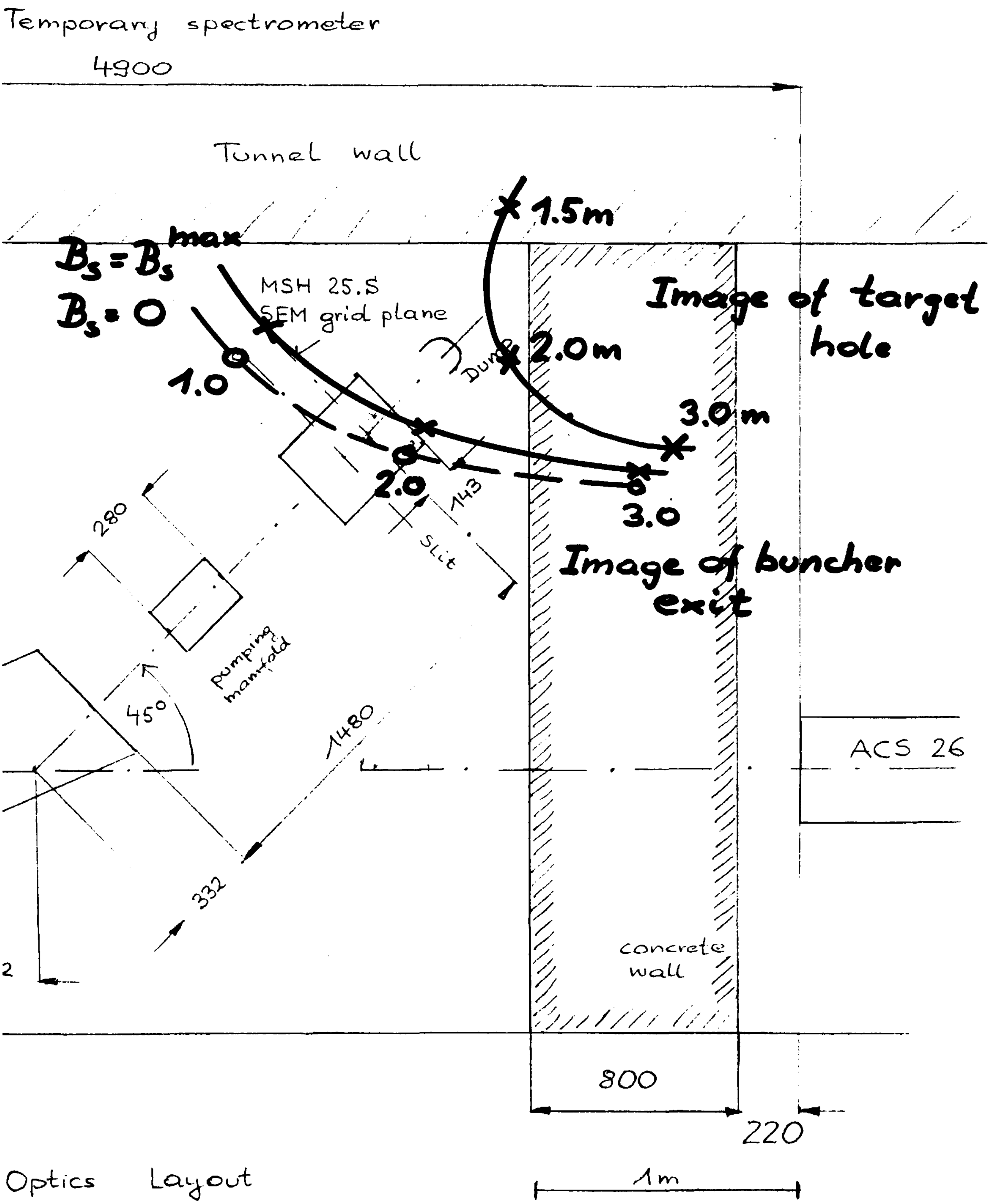

Optics Layout

9.10.85
K. Hübner

Fig.2

9.10.85

Phase plane at SEM grid

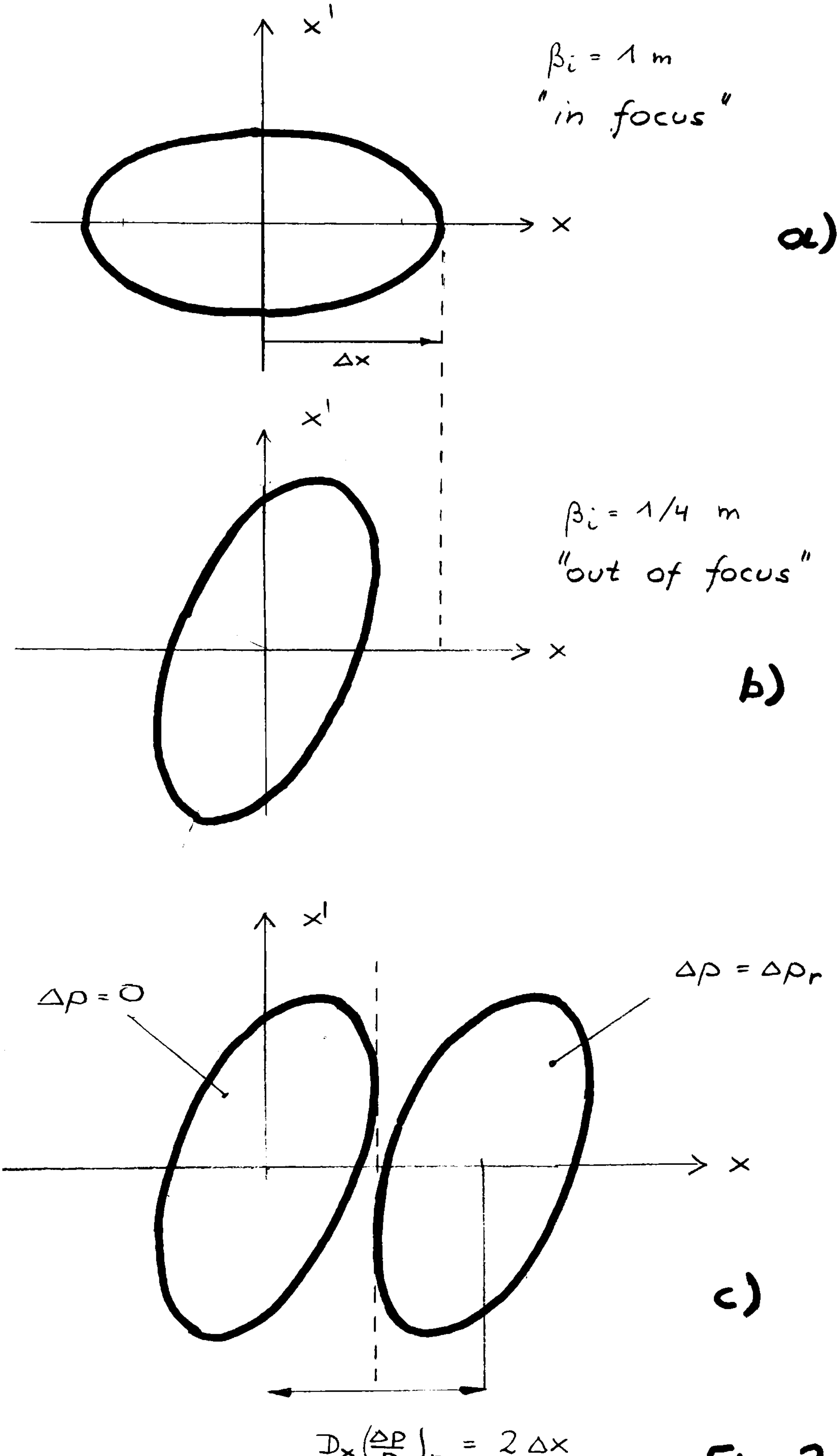

Fig. 3

4.9.85

Horiz. beam radius at SEM-grid

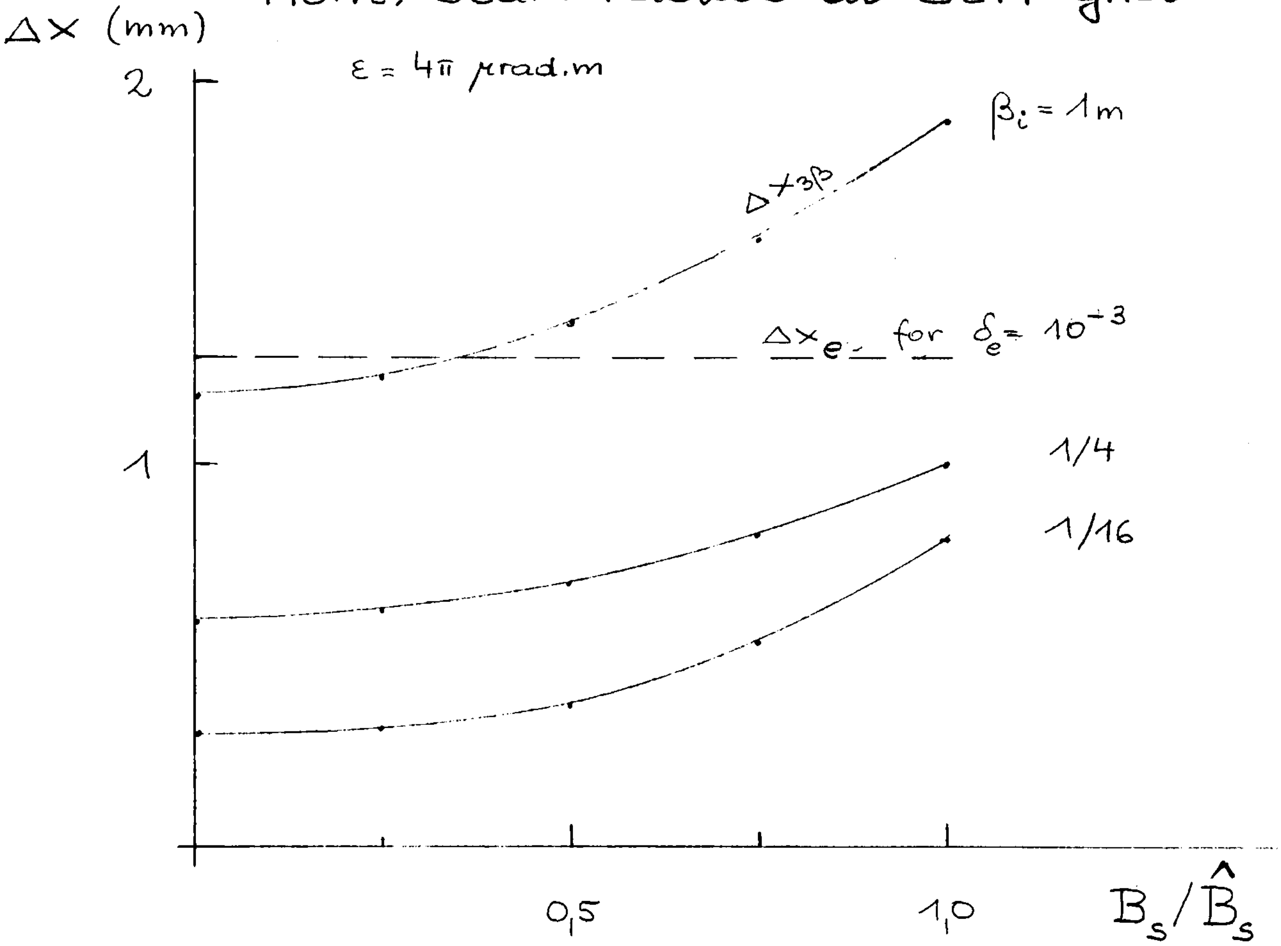

Fig. 4

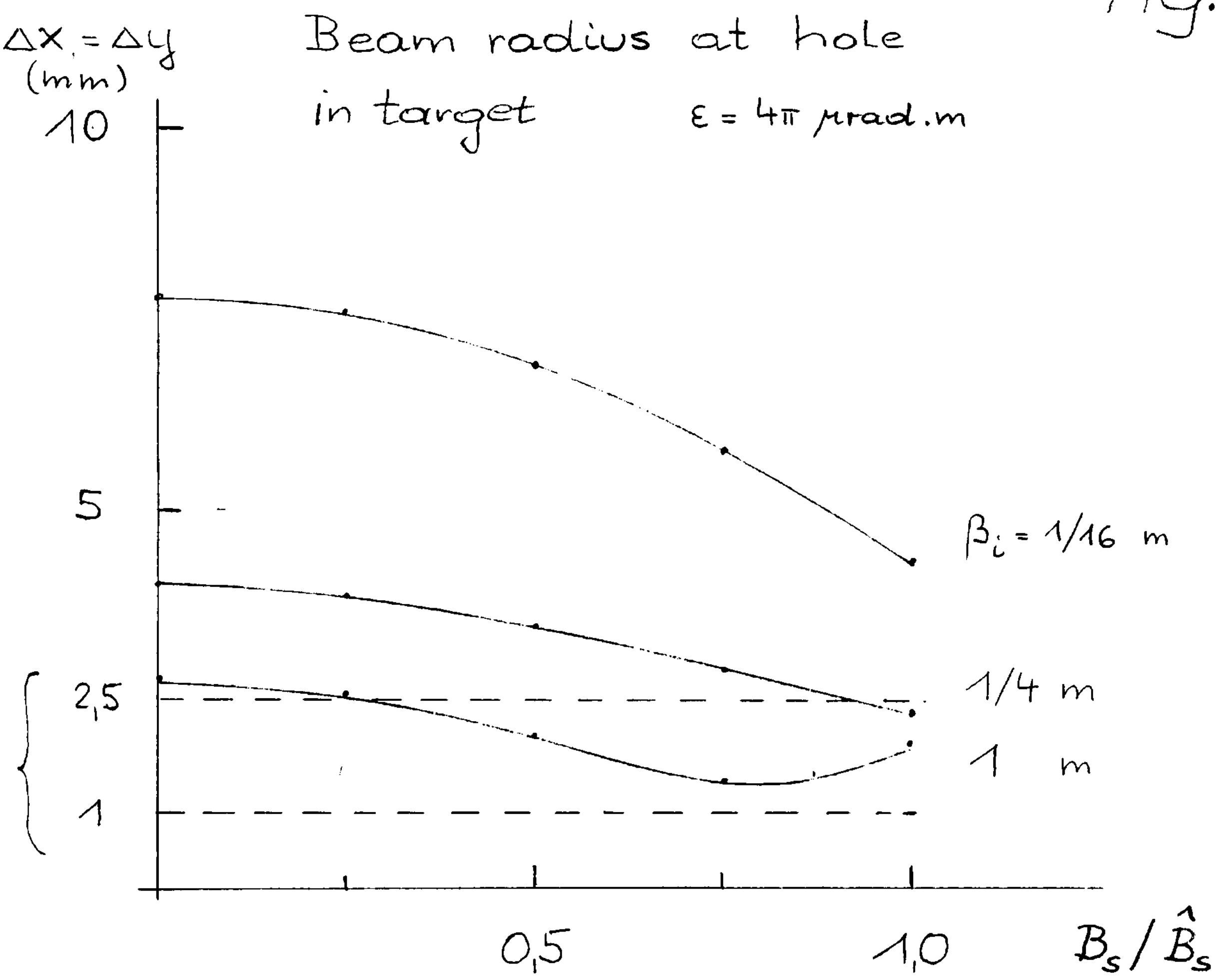

SNT 25 Solenoid strength

Fig. 5 II

11.10.85

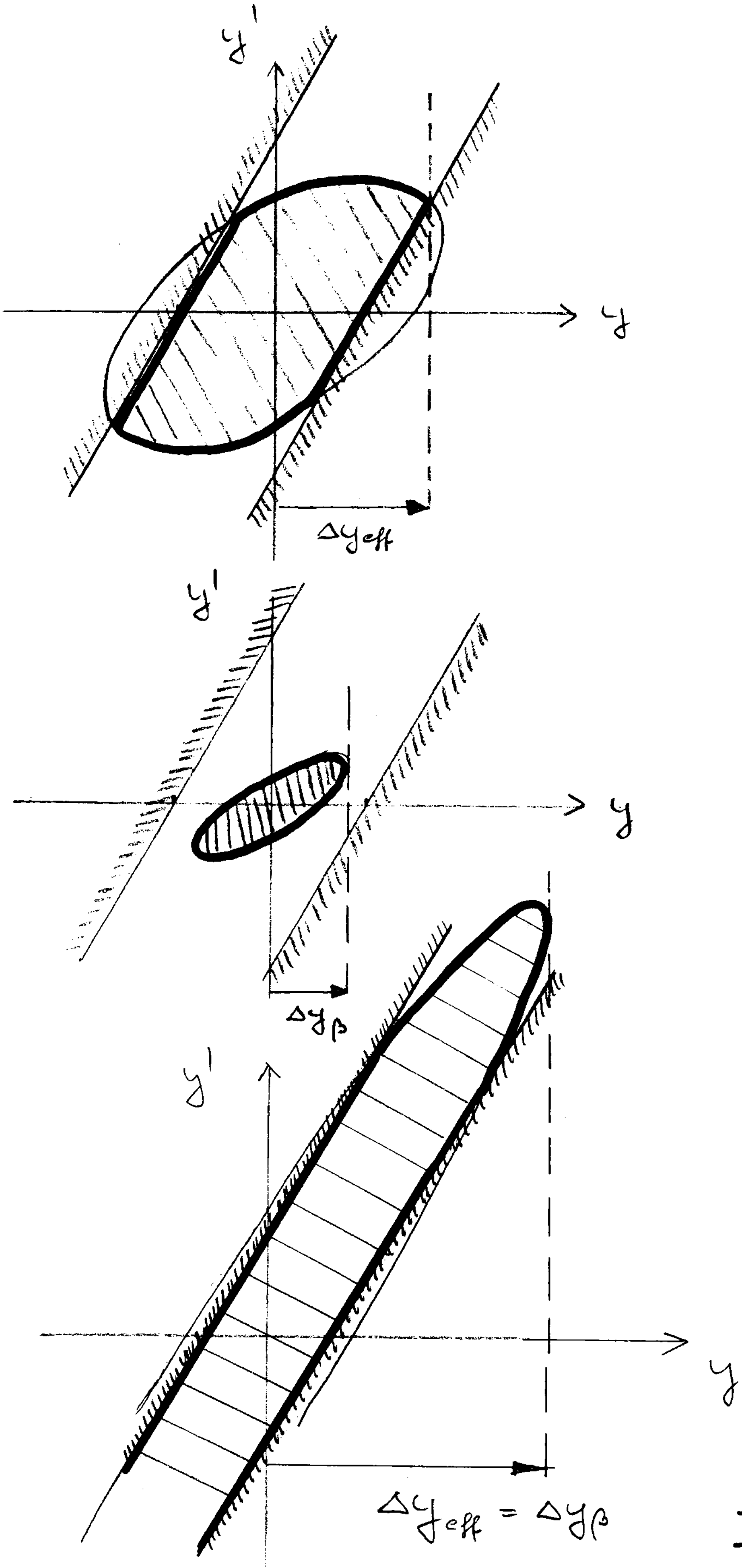

Fig. 6

Vertical beam radius at SEM grid MSH 25.S

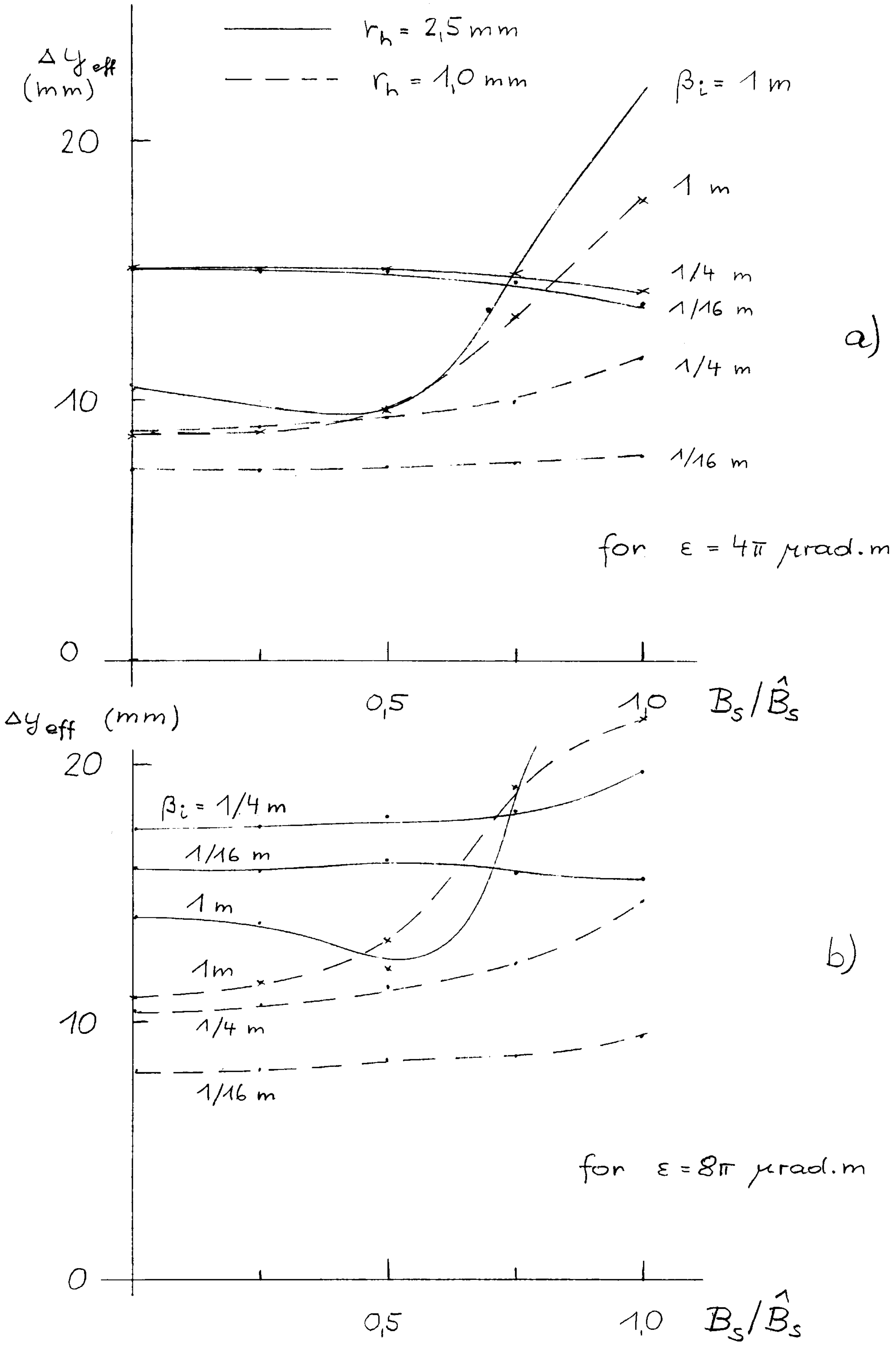

SNT25 Solenoid strength

Fig.7

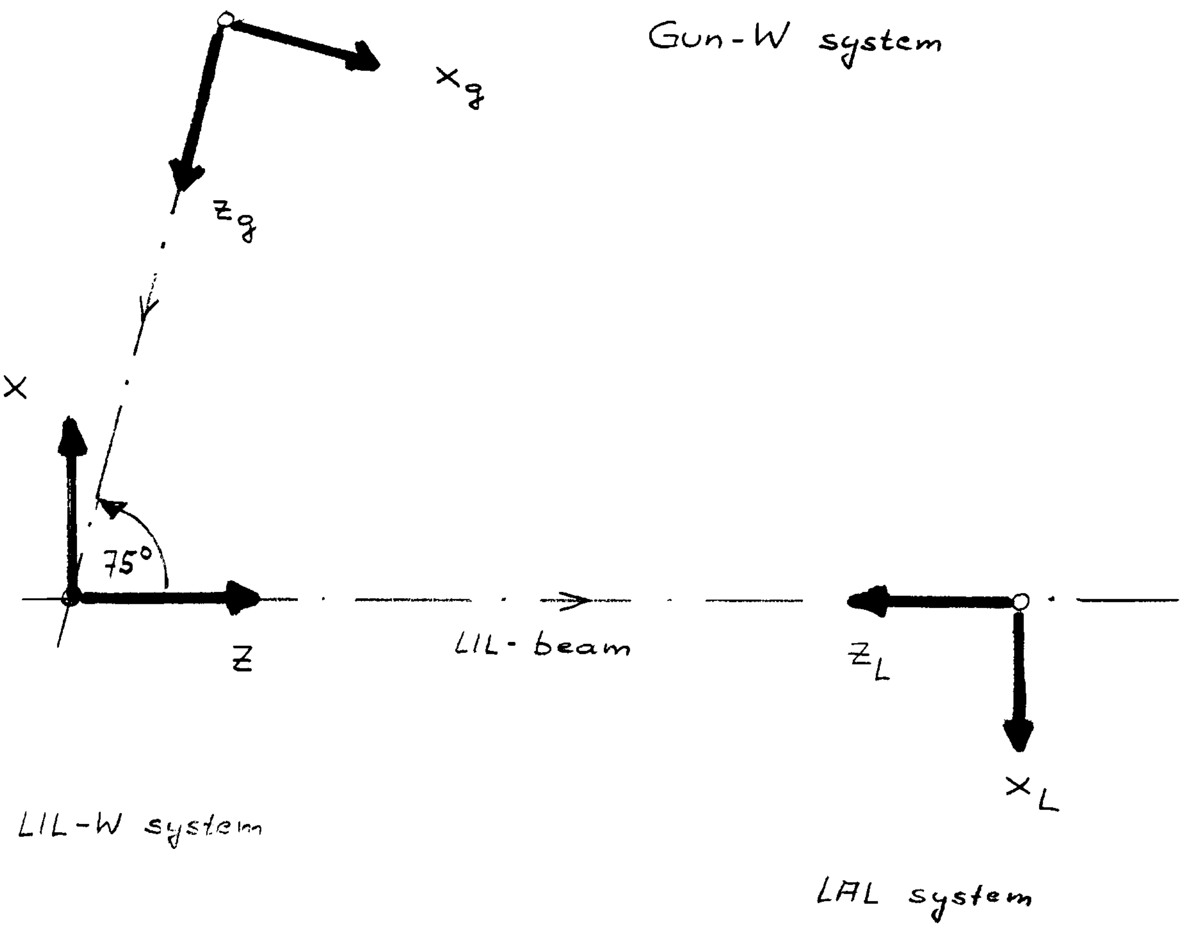

Fig. 8 Accelerator coordinate systems